First-principles investigation of the optical properties of crystalline poly(di-*n*-hexylsilane)

W. Y. Ching and Yong-Nian Xu
Department of Physics, University of Missouri–Kansas City, Kansas City, Missouri 64110

R. H. French
Du Pont Company, Central Research, E356-323, Experimental Station, Wilmington, Delaware 19880
(Received 15 March 1996; revised manuscript received 8 July 1996)

The optical properties of poly(di-*n*-hexylsilane) are studied by first-principles local-density calculations based on the crystal structure recently determined by x-ray diffraction. The one-dimensional nature of the band, the orbital composition of the states, the charge distribution of the highest-occupied-molecular-orbitals–lowest-unoccupied-molecular-orbitals states on the Si backbone, the effective masses, and the anisotropic optical conductivity are all clearly delineated. [S0163-1829(96)04543-2]

I. INTRODUCTION

Polysilanes are σ-conjugated high polymers with a Si backbone and carbon-based side groups. Because of their remarkable linear and nonlinear optical properties that may have potential applications, research on polysilanes and their derivatives has been the top agenda of many polymer chemists and physicists.[1] Among them, the poly(di-*n*-hexylsilane) (Pdn6s), which has two side chains of six methylene units each, is probably the most well studied. The observation of thermochromism,[2] a reversible change in the absorption band from 313 to 374 nm with a transition temperature of 40 °C, has attracted a tremendous research interest in the structure and properties of Pdn6s and other polysilanes. The change in the vacuum ultraviolet (UV) spectrum of Pdn6s with temperature is believed to be due to a change in the Si backbone conformation which changes the electronic structure and the long-wavelength absorption.[2] The large optical absorption in the UV region[3,4] and the observations of one photon, two photon absorptions,[5] third-order optical nonlinearity,[6] exciton-exciton annihilations,[7] and photo-induced birefringence are all believed to be associated with the delocalized nature of the lower conduction band (CB) states. Also significant is the complex interplay of the one-dimensional (1D) nature of the Si backbone versus the 3D nature of the polymer crystal stabilized by substantial interaction between the polymer side chains. Understanding the fundamental electronic structure of Pdn6s and other polysilanes and their remarkable optical properties is a subject of high current interest. One of the central issues is the following: are the optical properties of polysilanes best described by a many electron correlated model,[8] or the one-electron band theory.[9] Another important problem is whether the first strong peak observed in the UV spectrum is excitonic in origin or can be attributed to band-to-band transitions with unusually large oscillator strength. There have been numerous theoretical calculations on polysilanes.[8–14] Early work based on empirical models provided much of the insight,[15] but were less precise because of the difficulty in treating the self-consistent field effect and the interchain interactions. Molecular-orbital calculations[16] on a single polymer molecule have difficulty in treating the dispersion forces between the nonbonded part of the extended molecule. The band-structure approach is more appealing in the sense that it can include the intermolecular interactions. Champagne and André calculated the longitudinal linear polarizability of polyethylene and polysilane chains using an *ab initio* method equivalent to uncoupled Hartree-Fock method.[13] Mintmire[9] performed first-principles calculations on polysilanes for the 1D band structures and optical absorption spectra on models of different backbone conformations and alkyl substitutions. However, the calculated amplitude of absorption was too small. Takeda and Shiraishi[11] used a local-density-approximation (LDA) pseudopotential-Gaussian method to study the electronic structure of 1D and 2D Si-skeleton materials in which all the alkyl side chains are substituted by H atoms. These theoretical calculations were hindered by the lack of precise structural information for the polymer crystals and the conclusions thus obtained were more general in nature.

Recently, the crystal structure and atomic coordinates of Pdn6s were determined by Patnaik and Farmer[17] using x-ray diffraction techniques. An orthorhombic cell (space group $Pn_{na}2_1, Z=2$) with lattice constants $a=13.76$ Å , $b=23.86$ Å , and $c=3.99$ Å was obtained. This is in contrast to the earlier study[18] which gave a triclinic cell. A 2D projection of the unit cell on to the *a*-*b* plane is shown in Fig. 1. The Si backbone chain along the *z* axis was found to be in all-*trans* form but the alkyl side chains are not all-*trans* and are not normal to the Si backbone. This more complex structure apparently minimizes the intramolecular interaction and enhance the intermolecular interaction for stabilizing the all-*trans* backbone conformation.[17]

In this paper, we report the results of a first-principles investigation of the electronic structure and the optical properties of Pdn6s based on the newly determined 3D crystal structure. Our calculations provide the state densities and their orbital components in the entire valence-band (VB) region. Calculation of optical properties including the full matrix element effects enables us to explain the the major features of the observed UV optical spectrum for frequencies up to 32 eV. Based on the band structure and the analysis of the wave functions, a clear and consistent picture of the fundamental electronic properties of Pdn6s has emerged. We

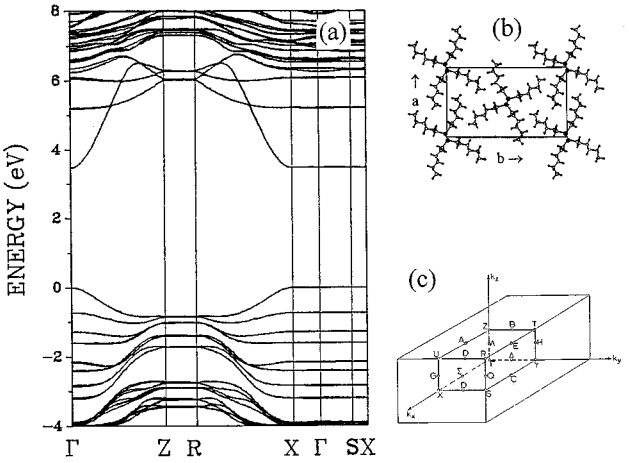

FIG. 1. (a) Calculated band structure of Pdn6s crystal. (b) Projection of the Pdn6s crystal on the *a*-*b* plane (from Ref. 15): ●, Si; ○, C; ·, H. (c) Brillouin zone of the crystal.

briefly describe our method of calculation in the following section. Section III is then devoted to the discussion of the results with a brief conclusion at the end.

II. METHOD OF CALCULATION

We used the orthogonalized linear combination of atomic orbitals (OLCA) method[19] to calculate the electronic structure of the Pdn6s crystal. This is an all-electron fully self-consistent method based on the LDA of the density-functional theory (DFT), and is known for its efficiency and accuracy especially for complex crystals. The density-functional theory[20,21] provides the formal theoretical justification for reducing a many-electron problem to a single particle form. In this theory, the ground-state electron density distribution $\rho(\mathbf{r})$ is the fundamental quantity and can be obtained as the sum of the squares of the occupied Kohn-Sham orbitals.[22] The ground-state energy is a unique function of $\rho(\mathbf{r})$ and contains the exchange-correlation contribution $E_{\mathrm{xc}}[\rho(\mathbf{r})]$ whose exact functional form is unknown. In the local approximation and making use of the result for an interacting homogeneous electron gas, the exchange part of the potential can be shown to be $V_x(\mathbf{r}) = -(\frac{2}{3})\times 6[3\rho(\mathbf{r})/8\pi]^{1/3}$. Additional correlation effect in the form of, for example, Wigner interpolation[23] or Ceperley and Alder form[24] may be added. The single-particle Kohn-Sham equations are solved self-consistently. The local approximation makes the DFT-based methods extremely versatile for electronic structure studies of large systems in condensed matter and materials research. In recent years, there have been many concerted efforts in improving the DFT/LDA methods and in applying them to systems of greater complexity.[25]

The unit cell of Pdn6s contains 4 Si, 48 C, and 104 H atoms for a total of 312 valence electrons. The basis functions are atomic orbitals consisting of the core and the valence orbitals of Si, C, and H expressed as combinations of Gaussian-type orbitals (GTO). To improve the CB states, Si 4*s*, and 3*d* orbitals were also included in the basis set. The crystal potential and the charge density were expressed as atom-centered functions consisting of GTO and iterated to self-consistency via the solution of one-particle Kohn-Sham equations. The Wigner interpolation formula was used to account for additional correlation effects. Two- and three-center interaction integrals were evaluated as far as necessary with no truncations. Because the unit cell is large and the system is insulating, test calculations show that using only the Γ point for the self-consistent iteration is very adequate. Convergence in the potential was obtained in less than 20 iterations when the eigenvalues stabilize to less than 0.0001 eV in the differences. The final calculations of the density of states (DOS) and optical properties were based on the energy eigenvalues and wave functions obtained at 20 regularly spaced **k** points within $\frac{1}{8}$ of the Brillouin zone (BZ).

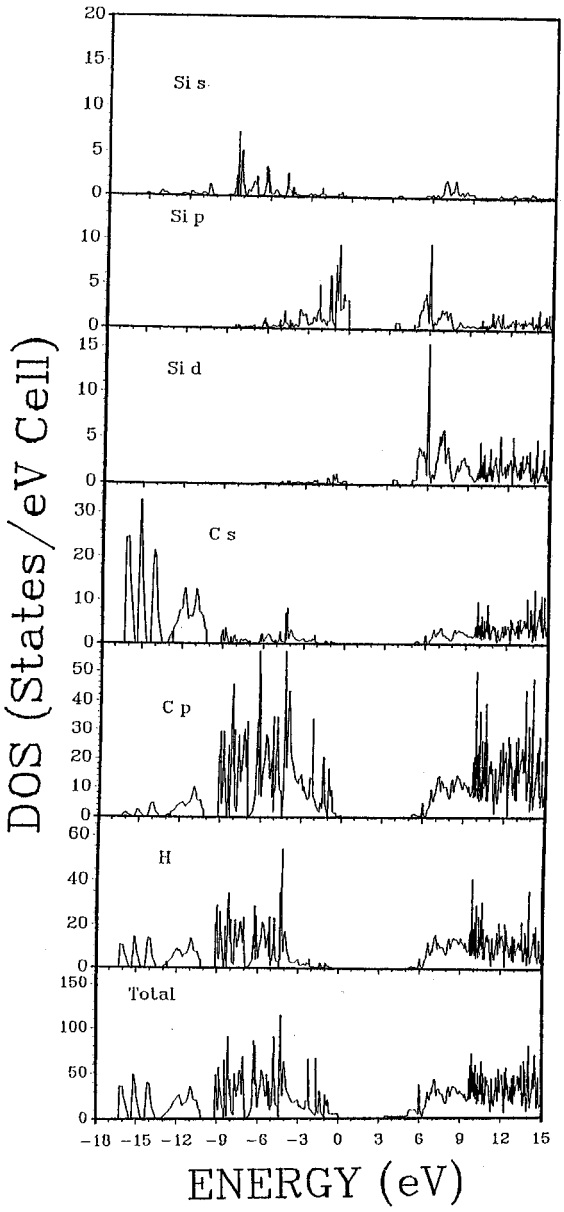

FIG. 2. The calculated total DOS and orbital-resolved partial DOS of Pdn6s. Note the difference in the scale for each panel.

III. RESULTS AND DISCUSSION

Figure 1 shows the calculated band structure of Pdn6s along the symmetry axis of the orthorhombic BZ. A direct

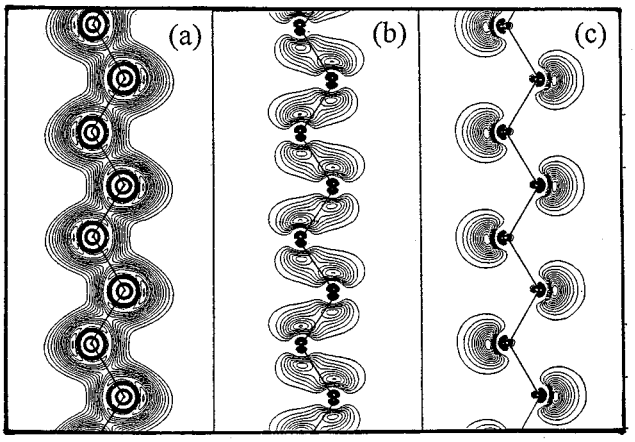

FIG. 3. Distribution of the charge on the Si backbone in Pdn6s. (a) Total valence charge; (b) the HOMO state at Γ; and (c) the LUMO state at Γ. The contour lines are in the unit of 0.01 to 0.25 by 0.005 electron for (a), and 0.0 to 0.6×10^{-3} by 0.2×10^{-4} electron for (b) and (c).

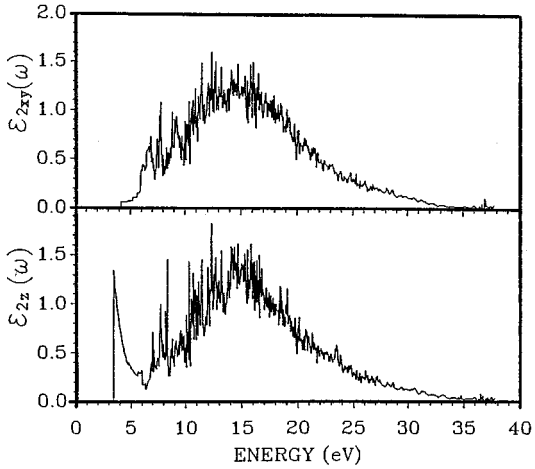

FIG. 4. The calculated $\varepsilon_2(\omega)$ of Pdn6s. (a) $\parallel$ to z direction; (b) $\perp$ to chain direction.

LDA band gap of 3.5 eV at Γ is obtained that is consistent[26] with the experimental gap of about 4.0 eV.[3,4] The good agreement between the calculated LDA gap and the measured gap is probably due to the rather compact basis set used in the present calculation. All the states in the VB and the lower CB are nearly degenerate because there are two polymer chains in the unit cell. This degeneracy is gradually removed for the more delocalized higher CB due to interchain interaction. The most prominent feature of Fig. 1 is the 1D Si backbone band of width 2.52 eV in the k_Z direction (Γ to Z). There is very little band dispersion in the k_x-k_y plane. The 1D CB crosses three other bands with the first crossing occurring near the midpoint of the Γ-Z axis. In accordance with convention, we label the top of the VB at Γ as the HOMO (highest occupied molecular orbital) state and the lowest CB at Γ as the LUMO (lowest unoccupied molecular orbital) state. From the band curvatures, it was determined that the hole and electron effective masses along the k_z direction for the HOMO and LUMO states are -0.42 m and 0.19 m, respectively, which fall within the range of typical semiconductors. This implies that carrier transport in the Pdn6s crystal is along the Si backbone chain as expected, and is consistent with the observation of mobile hole photoconduction in polysilanes.[27]

The electronic structure of Pdn6s can best be illustrated by the DOS and its partial components (PDOS) are shown in Fig. 2. From the PDOS it is clear that while the HOMO state is predominantly derived from the Si 3*p* orbitals with a small C 2*p* mixing, the LUMO state contains significant mixing of Si 3*d* orbitals. This is in contrast to the molecular-orbital calculations[10] which shows Si 3*d* to be inconsequential in the unoccupied levels. The CB PDOS also show a very sharp peak at 6 eV with a strong Si *p*-*d* mixing. This peak corresponds to the very flat band at 6 eV. The Si 3*d* PDOS is quite significant in the CB region up to 9.5 eV. Although our basis functions appear to have an over-description for the Si 3*d* component with respect to the C and H atoms, our results do indicate that Si 3*d* orbitals play an important role in the UV spectrum of Pdn6s. Also evident from Fig. 2 is that in the VB region, Si states are limited to above -9 eV. The three lowest peaks at -16.1, -15.0, and -14.0 eV are from C-H bonding. The H states are limited mainly to below -3.5 eV. The C 2*s* and C 2*p* states dominate the regions below -10 eV and above -9 eV, respectively. They interact significantly with H and Si in the respective energy ranges. This result shows it is insufficient to use H-terminated Si chains as the representative structure of polysilanes.

Figure 3(a) shows the total valence charge density in the plane containing the zigzag Si backbone. The strong covalent bonding between Si atoms and the confinement of the charge to the backbone are obvious. Figures 3(b) and 3(c) show the charge distributions of the HOMO and LUMO states in the same plane. For the HOMO state, the strong covalent bonding of the Si 3*p* orbitals is evident. The lobe structure indicates the bonding is not strictly along the Si-Si chain direction. Inspection of the wave function shows it is mostly from the Si 3*pz* orbital. Most likely, it is influenced by the charges present in the side chains. The distribution of the LUMO state shows the antibonding character of a highly delocalized state with admixture of Si 3*s*, Si $3p_y$, and Si $3d_{3z^2-r^2}$ orbitals. The lobes are directed perpendicular to and away from the Si backbone chain. The orbital characteristics of the HOMO and the LUMO states signify a strong symmetry-allowed transition leading to a large optical matrix element at Γ. Champagne and André[13] had also found in their study of polysilane chain, that the HOMO state is at the Γ point and its structure is mainly composed of the Si 3*p* orbitals in the direction of the chain. Effective charge calculation using the Mulliken scheme[28] shows that each Si loses 0.51 electron to the adjacent C atoms. Each C atom at the ends of the side chains also gains a charge of 0.70 electron at the expense of the three bonding H. On average, each Si backbone within the unit cell loses about one electron to the side chains. This again demonstrates the importance of having the correct crystal structure for polysilane calculations. It should be pointed out that effective charge calculation based on the

Mulliken scheme is only qualitative and may be somewhat basis dependent.

The calculated imaginary part of the frequency-dependent dielectric function $\varepsilon_2(\omega)$ is shown in Fig. 4. The calculation includes the full evaluation of the transition matrix elements at each **k** point. We resolve the $\varepsilon_2(\omega)$ into parallel (to the z direction) and perpendicular components. The optical anisotropy is very strong especially in the frequency region above the gap which leads to optical birefringence. The most striking feature is the sharp leading peak with a very steep edge at 3.5 eV in the parallel component. This is clearly the strong $\sigma \rightarrow \sigma^*$ transition from HOMO to LUMO at the zone center. The rapid decrease in amplitude of this peak from 3.5 to 6 eV is the signature of the 1D band shown in Fig. 1. There are other peaks in the 6–11-eV range. The main broad peak in the calculated curve is at 14 eV. The position of the main peak is believed to be overestimated due to the use of a minimal basis sets for C and H which constitute the alkyl side chains. If a sufficiently large basis is used, the higher CB states are expected to be pushed down, resulting in the shifting of the main peak to lower energy.

The optical properties of polysilanes have been determined by reflectance and transmission measurements from the near infrared to the vacuum UV and soft-x-ray region (0.5–44 eV).[3,4] The complex dielectric functions were completely determined by Kramers-Kronig (KK) analysis. The experimentally derived $\varepsilon_2(\omega)$ for Pdn6s is shown in Fig. 5. The main features are a very sharp E_1 peak at 3.39 eV, a sharp peak E_1' at 4.0 eV, an E_2 peak at 7.1 eV, and a broad peak at 9.4 eV. It was suggested[5] that transitions in the 3–5 eV is from the $\sigma \rightarrow \sigma^*$ backbone transition, that in the 5–8 eV region is from the backbone to the side chain transition, and transitions above the 8 eV involve alkyl side chains. To compare with the theoretical calculation, we plot in Fig. 5 the smoothed average curve of Fig. 4. To simulate the effect of an enlarged basis set, we compressed the theoretical curve in a nonlinear fashion such that the main peak is more or less aligned with the experimental one with the total area under the curve preserved. Spectral data at the higher-energy range are compressed more than the lower-energy ones. The agreement between the two curves is quite impressive in terms of the general sharp, structures, and amplitudes. Our calculation shows only one strong peak at the absorption edge which must be identified as the E_1' peak at 4 eV since the LDA calculation generally underestimates the band gap. The observed sharp E1 peak must therefore be excitonic in origin.

The problem of 1D exciton (or equivalently, the 1D hydrogen atom) has a long history of interest to mathematical physicists.[29] It is of relevance to several physical systems such as quantum wires, or atoms and semiconductors in high magnetic field. For a pure 1D exciton with an infinite range of Coulomb interaction, the ground state is unbounded. The 1D or 3D nature of the exciton in the polysilane system is not totally clear. Although the band structure shows a strong 1D character, the crystal itself is three-dimensional and the HOMO-LUMO wave functions have finite extent in the x-y plane. The range of interaction in the LDA calculation is also finite. Assuming the ground-state exciton in polysilane is bounded and the complicated many-body effect can be

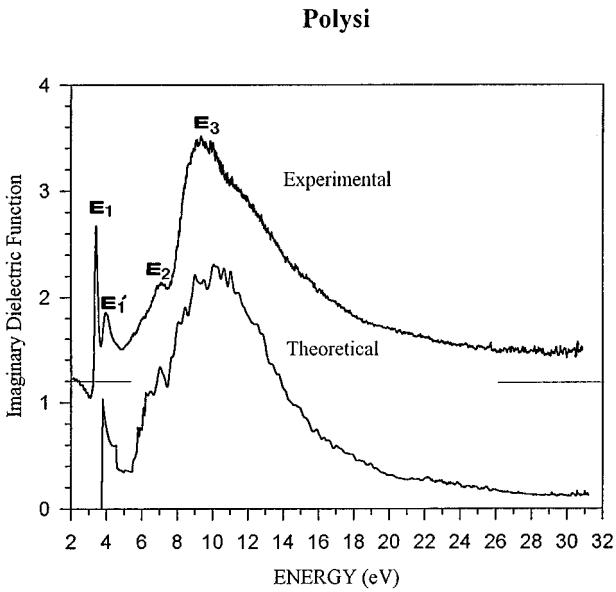

FIG. 5. Comparison of the measured (upper) and calculated (lower) $\varepsilon_2(\omega)$ curves. The theoretical curve has been compressed towards the lower energy to simulate the effect of an extended basis.

partially absorbed by the dielectric screening, the binding energy E_B of the exciton in Pdn6s may be roughly estimated. It turns out that the expression for E_B for a 1D exciton is exactly the same as for the 3D exciton,[30] but the same cannot be said to the 2D exciton. In 2D, E_B is four times as large as in 3D.[31] The effective masses of the HOMO-LUMO states give a reduced effective mass of the electron-hole pair to be $\mu^* = 0.13$ m. The static dielectric constant of $\varepsilon_0 = 2.1$ is obtained as the zero frequency limit of the real part of the calculated dielectric function obtained from $\varepsilon_2(\omega)$ by KK conversion. We obtained a binding energy of 0.41 eV which is not too far from the separation of the E_1 and E_1' peaks (0.61 eV) in the experimental vacuum UV spectrum.

In conclusion, the LDA-based first-principles band approach is very effective in elucidating the structure and properties of the polysilane polymers. The present calculation delineates the nature of bonding in one such polymer and unequivocally show that optical properties in the UV region are mainly controlled by the orbital bonding of the Si backbone. It is thus expected that different backbone confirmation can change the HOMO and LUMO state levels and wave functions to give different optical spectra. This is consistent with the notion that thermochromism in Pdn6s is associated with an order-disorder transition from an all-*trans* to a one at least partly *trans-gauche*, with the accompanied variations in the structural arrangements of the side chains. This certainly affects the formation of bond exciton below the CB edge. The present calculation also demonstrates for that the Si 3*d* orbitals are important in the unoccupied states which determine the optical properties in the UV region.

ACKNOWLEDGMENTS

We thank Dr. S. S. Patnaik and Dr. B. L. Farmer for providing the coordinates of the Pdn6s crystal. R.H.F. thanks Dr. F. M. Schellenberg, Dr. R. D. Miller, Dr. R. M. Hochstrasser, Dr. J. S. Meth, and Dr. J. R. G. Thorne for past collaborations on the subject. W.Y.C. thanks Dr. K. W. Wong and Dr. F. T. Chan for discussion on the structures of low-dimensional excitons. The work at UMKC was supported by DOE Grant No. DE-FG02-84DR45170.

[1] R. D. Miller and J. Michl, Chem. Rev. **89**, 1359 (1989); R. West, J. Organomet. Chem. **300**, 327 (1986).

[2] R. D. Miller, D. Hofer, J. Rabolt, and G. N. Fickes, J. Am. Chem. Soc. **107**, 2172 (1985).

[3] F. M. Schellenberg, R. L. Byer, R. H. French, and R. D. Miller, Phys. Rev. B **43**, 10 008 (1991).

[4] R. H. French, J. S. Meth, J. R. G. Thorne, R. M. Hochstrasser, and R. D. Miller, Synth. Met. **49-50**, 499 (1992).

[5] H. Tachibana, M. Matsumoto, Y. Tokura, Y. Moritomo, A. Yamaguchi, S. Koshihara, R. D. Miller, and S. Abe, Phys. Rev. B **47**, 4363 (1993).

[6] F. Kajzar, J. Messier, and C. Rosillio, J. Appl. Phys. **60**, 3040 (1986); H. Kishida *et al.*, Phys. Rev. B **50**, 7786 (1994); Phys. Rev. Lett. **47**, 9253 (1993).

[7] R. G. Kepler and Z. G. Sos, Phys. Rev. B **47**, 9253 (1993).

[8] Z. G. Soos and G. W. Hayden, Chem. Phys. **143**, 199 (1990).

[9] J. M. Mintmire, Phys. Rev. B **39**, 13 350 (1989).

[10] J. Michl, Synth. Met. **49-50**, 367 (1992); V. Balaji and J. Michl, Polyhedron **10**, 1265 (1991).

[11] K. Takeda and K. Shiraishi, Phys. Rev. B **39**, 11 028 (1989); K. Takeda, K. Shiraishi, M. Fujiki, M. Kondo, and K. Moigaki, *ibid.* **50**, 5171 (1994).

[12] K. Seki, T. Mori, H. Inokuchi, and K. Murano, Bull. Chem. Soc. Jpn. **61**, 351 (1988); N. Matsumoto and H. Teramae, J. Chem. Soc. **113**, 4481 (1991).

[13] B. Champagne and J. M. André, Int. J. Quantum Chem. **42**, 1009 (1992).

[14] E. Ortiu *et al.*, Synth. Met. **57**, 4419 (1993).

[15] C. Sandorfy, Can. J. Chem. **33**, 1337 (1955).

[16] J. R. Damewood, Jr., Macromolecules **18**, 1793 (1985); B. L. Farmer, J. F. Rabolt, and R. D. Miller, *ibid.* **20**, 1167 (1987).

[17] S. S. Patniak and B. L. Farmer, Polymer **33**, 4443 (1992).

[18] H. K. Kuzmany, J. F. Rabolt, B. L. Farmer, and R. D. Miller, J. Chem. Phys. **85**, 7413 (1986).

[19] W. Y. Ching, J. Am. Ceram. Soc. **73**, 3135 (1990).

[20] P. Hohemberg and W. Kohn, Phys. Rev. **136**, B864 (1964).

[21] W. Kohn and L. J. Sham, Phys. Rev. **140**, A1133 (1965).

[22] L. J. Sham and W. Kohn, Phys. Rev. **145**, 561 (1966).

[23] E. Wigner, Phys. Rev. **46**, 1002 (1934).

[24] D. M. Ceperley and B. J. Alder, Phys. Rev. Lett. **45**, 566 (1980).

[25] See, for example, *Density Functional Theory of Molecules, Clusters, and Solids*, edited by D. E. Ellis (Kluwer Academic, Boston, 1995).

[26] It is well known that LDA calculations generally underestimate the band gap of insulators. Gap correction procedures based on an approximate GW quasiparticle approach within the OLCAO scheme has been devised [see Z.-Q. Gu and W. Y. Ching, Phys. Rev. B **49**, 10 958 (1994) and W. Y. Ching, Z.-Q. Gu, and Y.-N. Xu, *ibid.* **50**, 1992 (1994)]. However, it was not implemented in the present study since the main change is a rigid shift in the CB states with little effect on the single-particle wave functions. Also, a more rigorous calculation beyond LDA may have to wait until a LDA calculation with a more complete basis set is performed.

[27] R. G. Kepler, J. M. Ziegler, L. A. Harrah, and S. R. Kurtz, Phys. Rev. B **35**, 2818 (1987); M. Fujino, Chem. Phys. Lett. **136**, 451 (1987).

[28] R. S. Mulliken, J. Am. Chem. Soc. **77**, 887 (1954).

[29] W. Fischer, H. Lescnke, and P. Müller, J. Math. Phys. **36**, 2314 (1995).

[30] R. Loudon, Am. J. Phys. **27**, 649 (1959); L. K. Haines and D. H. Roberts, *ibid.* **37**, 1145 (1969).

[31] X. L. Yang, S. Guo, F. T. Chan, K. W. Wong, and W. Y. Ching, Phys. Rev. A **43**, 1197 (1991).